Colloid & Polymer Science Colloid Polym Sci 267:16–27 (1989)

Some novel crystallization kinetic peculiarities in finely dispersing polymer blends

H. Frensch and B.-J. Jungnickel

Deutsches Kunststoff-Institut, Darmstadt, F.R.G.

Abstract: The morphology and the crystallization of blends of poly(vinylidene fluoride) (PVDF) with polyamide-6 (PA-6), and with poly(butylene terephthalate) (PBTP), were investigated in detail by electron microscopy and by DSC. In some of the blends, the dispersed component exhibits rather small particle sizes and, followingly, a high number density of the dispersed particles which is in the order of magnitude of, or exceeds the number density of the usually nucleating heterogeneities. In these blends, the crystallization of the dispersed component proceeded in two steps, induced by different nucleating species ("fractionated crystallization"). The nuclei concentrations in the components and the specific interfacial energies of the PVDF nucleation steps were estimated. An unusual type of fractionated crystallization occurs in some cases: matrix and disperse phases crystallize completely coincident due to a specific mutual nucleating efficiency of both components. An estimation of the interfacial energies involved suggests a nucleating activity of PVDF crystals for PA-6. Moreover, a rise of the crystallization temperatures of the PA-6 and PBTP matrix phases is observed that may indicate a migration of nucleating impurities during melt processing from PVDF towards the second component.

Key words: Fractionated crystallization, polymer blends, nucleation, interface, infacial energies.

1. Introduction

Blending polymers is a promising way to new thermoplastic materials. The properties of these blends depend to a great extent on their supermolecular structure which in turn is influenced by the compatibility, by the processing history, and by the crystallization of the components as well. The latter, in particular, can alter remarkably in comparison to that of the pure materials. These changes can have different reasons, depending, again, on the mutual compatibility, on the differences of the glass transition and melting temperatures of the components, and on the actual crystallization temperature. For melt-compatible polymer blends, among other effects, a variation of the crystallization process due to altered nucleation and growth conditions has been reported [1–11]. A melting point depression has also been observed [1–5, 11, 12]. For polymer blends with extended interfacial regions these phenomena were reported to apply also to the transient layers [12–16]. The investigation of incompatible polymer blends also revealed changes of the crystallization of structural, equilibrium thermodynamic, and kinetic origin. Among other effects, the induction of specific crystal modifications [16], the rejection, engulfing, and deformation of the dispersed component by the growing spherulites of the matrix material [4, 17, 18], and nucleation at the interface [4, 19–22] have been reported. Polymer blends containing one component as finely dispersed droplet suspension exhibit sometimes the phenomenon of "fractionated crystallization" which originates in primary nucleation of isolated melt particles by units of different nucleating species [23–30]. This phenomenon resembles to some extent the classical droplet crystallization in which crystallization is inhibited until homogeneous nucleation occurs [31–35]. Fractionated crystallization proceeds stepwise at strictly different undercoolings, these steps sometimes being separated by more than 60 °C [23].

In this paper, we report on a novel kind of fractionated crystallization in which the second component acts as a nucleating agent. The influences of a lack of

nucleating heterogeneities, as well as of the interfacial properties of the system, on the crystallization kinetics are investigated and discussed. The polymer blends investigated are poly(vinylidene fluoride) (PVDF)/ polyamide-6 (PA-6), and PVDF/poly(butylene terephthalate) (PBTP).

2. Experimental part

As PVDF, Solef 1008 ($M_n = 38\,000$, $M_w = 100\,000$) from Solvay was used. The PA-6 that we used was Ultramid B3 ($M_n = 18\,000$) from BASF. Both substances were commercial grades. The PBTP of our investigations was Ciba Geigy PBT 85 Crastin, free of additives. The dried components were melt mixed at 230 °C in a single-screw laboratory extruder. The extruded strands were regranulated, and the extrusion cycle was repeated up to four times. After every cycle, samples were taken away for the investigations. By the repeated extrusion, different degrees of dispersion were realized.

The DSC measurements were carried out under nitrogen atmosphere. In order to destroy the self-seeding nuclei in the components, the samples were preheated for 5 min at 260 °C, this temperature being at least 35 °C above the melting points of the components. Then, the crystallization and reheating runs were performed at a standard rate of 10 °C/min. In some cases, other rates were used.

For the transmission electron microscopy (TEM), sections of (50...80) nm thickness were cryomicrotomed at −60 °C. For the scanning electron microscopy (SEM), the extruded strands were fractured in liquid nitrogen and sputter-coated with gold before examination.

Wide-angle x-ray scattering (WAXS) measurements using Cu-K_α-radiation, and torsion pendulum analysis at 1 Hz were performed too.

3. Results

3.1. Morphology

3.1.1. PVDF/PA-6 blends

In Figs. 1 and 2, TEM micrographs of unstained sections of PVDF/PA-6 blends are shown. The compo-

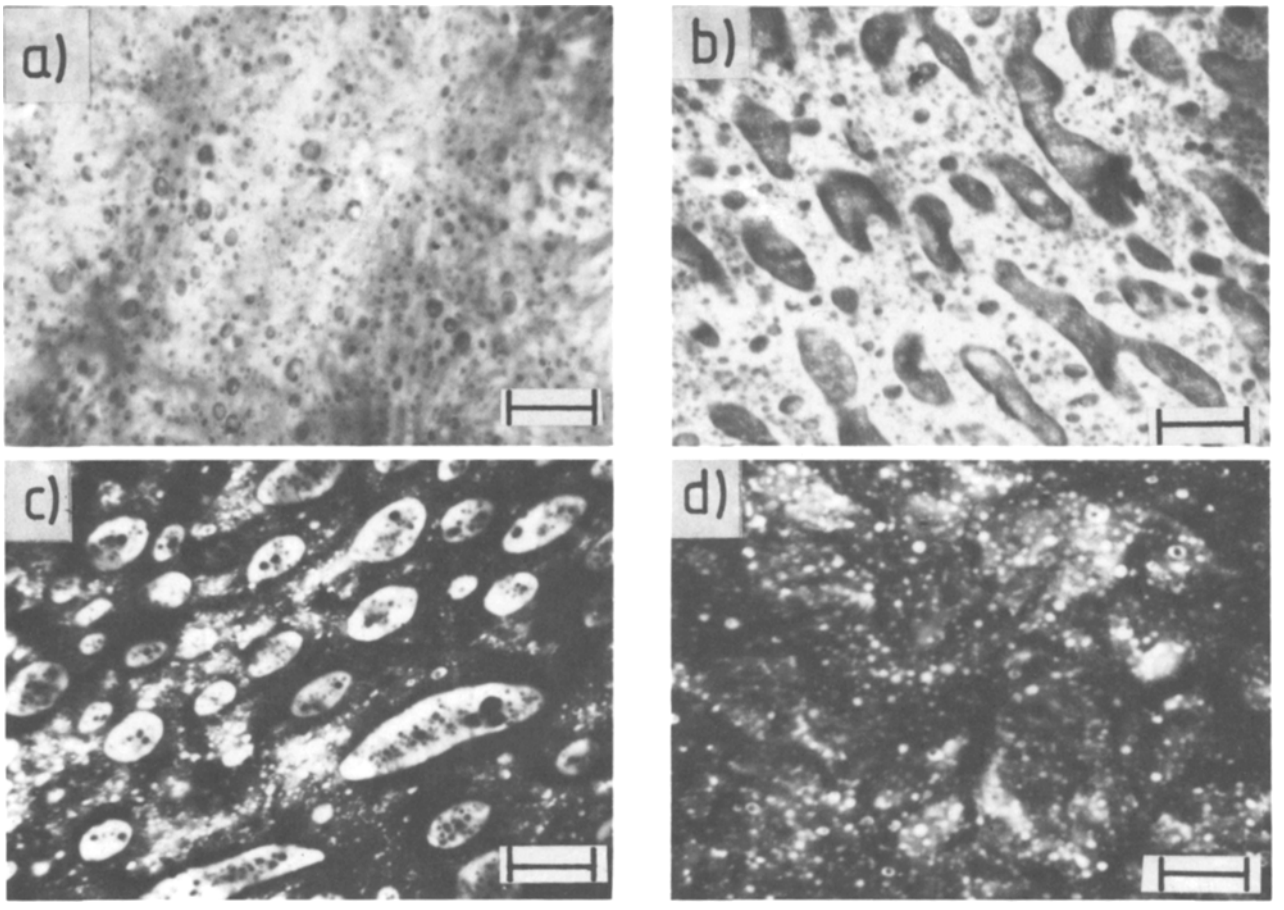

Fig. 1. Transmission electron micrographs of unstained thin sections of PVDF/PA-6 blends; four extrusion cycles; PVDF is the dark phase; scale bar corresponds to 2 μm. a) PVDF/PA-6 = 15/85 vol.-%; b) PVDF/PA-6 = 50/50 vol.-%; c) PDVF/PA-6 = 70/30 vol.-%; d) PVDF/PA-6 = 85/15 vol.-%

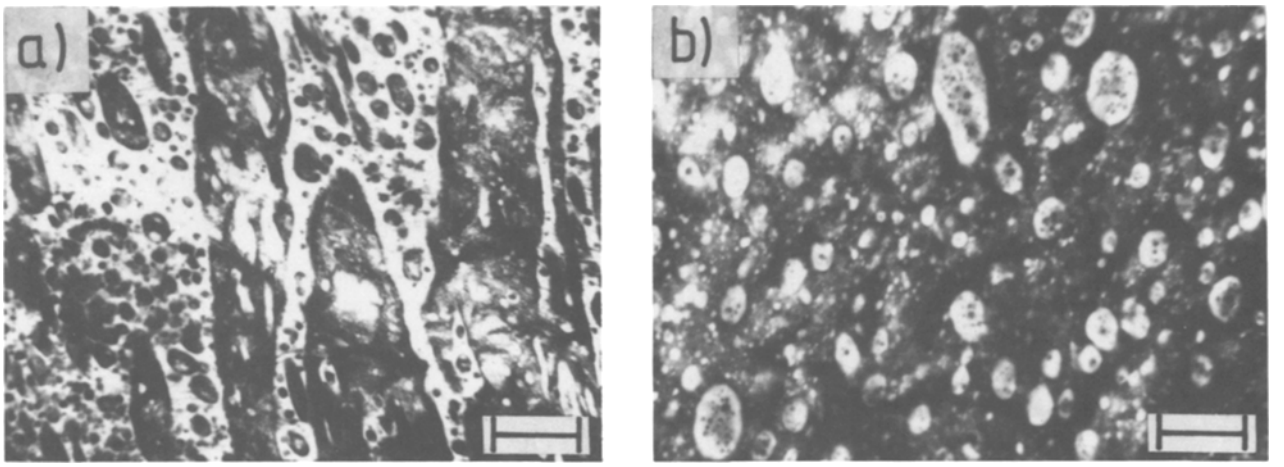

Fig. 2. Transmission electron micrographs of the PVDF/PA-6 = 75/25 vol.% blend; a) one extrusion cycle; scale bar represents 5 μm; b) four extrusion cycles; scale bar represents 2 μm

Table 1. Particle sizes

Sample	Extrusion cycle #	Displayed in Fig.	Particle diameters [μm]	
PVDF/PA-6				
[vol.-%]			PVDF	PA-6
15/85	4	1a	0.1 ... 0.6	matrix/0.05 ... 0.3 *i*
50/50	4	1b	0.2/2 *b*	matrix/0.05 ... 0.3 *i*
70/30	4	1c	matrix/0.2 *i*	2/0.05 ... 0.3 *b*
85/15	4	1d	matrix/0.2 *i*	0.05 ... 0.3
75/25	1	2a	matrix/0.2 ... 3 *i*	fibers/0.05 ... 2
75/25	4	2b	matrix/0.2 *i*	0.1 ... 1.6
PVDF/PBTP				
[vol.-%]			PVDF	PBTP
85/15	1	3a	matrix	0.7 ... 5
85/15	4	4a	matrix	0.1 ... 2
15/85	1	3b	1 ... 20	matrix
15/85	4	4b	0.7 ... 4	matrix

b = bimodal distribution with maxima at the given values; *i* = matrix material partly included with the given diameter into the particles of the dispersed component.

nents are phase separated. The PVDF phase appears dark probably due to its higher density and its content of fluorine atoms. The particle sizes are listed in Table 1.

Figure 1 displays blends of various compositions (four extrusion runs) which exhibit a very broad size distribution of the demixed particles, and, occasionally, a bimodal distribution with maxima in the μm and in the sub-μm range, respectively. Some of the greater particles, again, are composites in that sense that they contain, in their turn, particles of the matrix material as further level of dispersion.

In Fig. 2, the morphologies of two 75/25 blends are shown. After the first extrusion cycle (Fig. 2a), this blend exhibits globular as well as fibrillar particles of PA-6. Inside the PA-6 domains, PVDF particles are dispersed. After four extrusion cycles (Fig. 2b), the dispersed particles of the PA-6 became much smaller and did not further contain PVDF droplets.

The phase-separated structure as evaluated by TEM was confirmed by SEM. However, due to the different preparation techniques and modes of operation (TEM: sections; SEM: fracture surfaces) only the

TEM provided the contrast that was necessary to conclude on a certain component.

The torsion pendulum analysis of the blend exhibited discrete relaxations at the glass transition temperatures of PVDF and PA-6 at −45 °C and 50 °C, respectively. This also indicates incompatibility of the components after solidification, at least in the amorphous phase.

3.1.2. PVDF/PBTP blends

SEM of fracture surfaces of the system PVDF/PBTP revealed phase separation in this blend too (Figs. 3 and 4). The particles sizes (Table 1) are well above those in the respective PVDF/PA-6 blends. As for the system PVDF/PA-6, the particle diameter decreased with increasing extrusion cycle number. PBTP forms smaller particles than PVDF does in the reverse composition ratio.

3.2. Crystallization

3.2.1. PVDF/PA-6 blends

In Fig. 5, the crystallization of several four-times extruded PVDF/PA-6 blends as studied by DSC is dis-

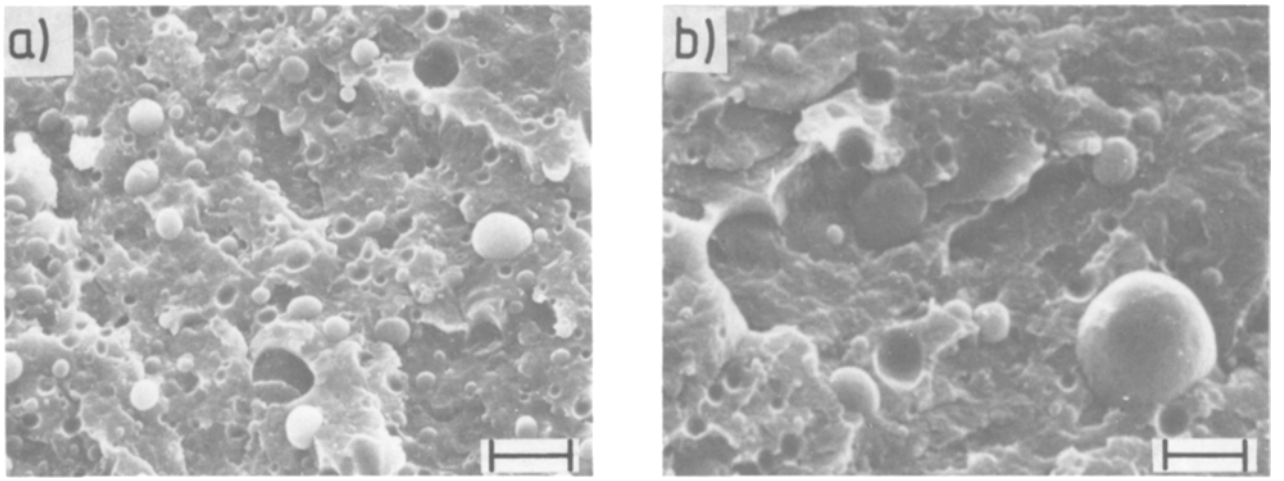

Fig. 3. Scanning electron micrographs of one-time extruded PVDF/PBTP blends; scale bar corresponds to 10 μm. a) PVDF/PBTP = 85/15 vol.-%; b) PVDF/PBTP = 15/85 vol.-%

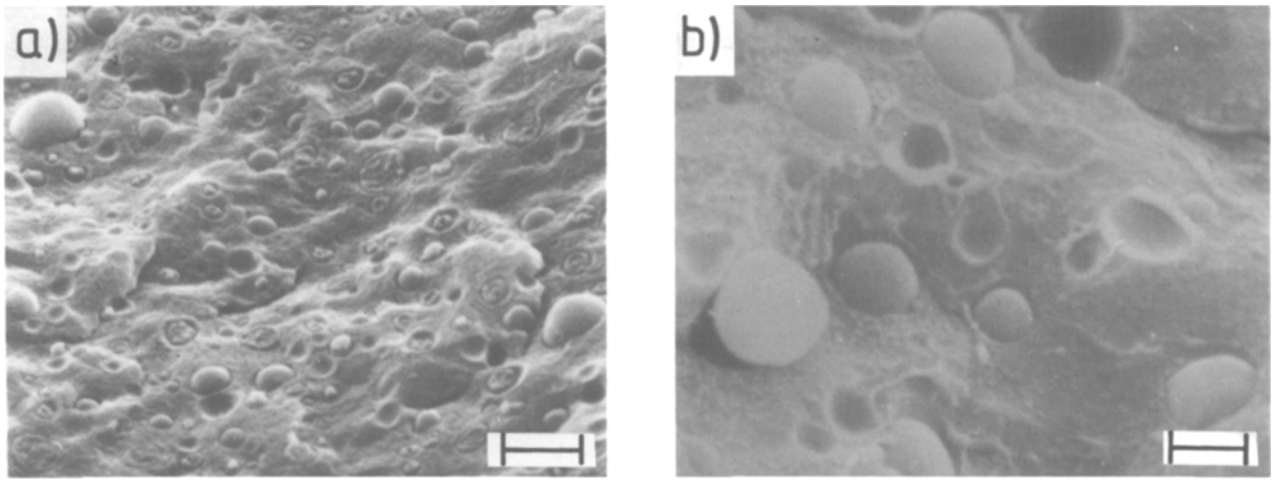

Fig. 4. Scanning electron micrographs of four-times extruded PVDF/PBTP blends; scale bar corresponds to 2 μm. a) PVDF/PBTP = 85/15 vol.-%; b) PVDF/PBTP = 15/85 vol.-%

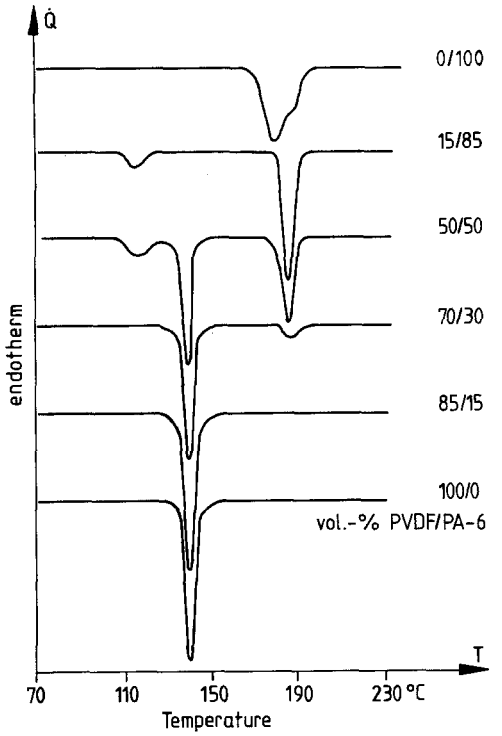

Fig. 5. DSC crystallization curves of PVDF/PA-6 blends. Four extrusion cycles; cooling rate: 10 °C/min

played (that is, for constant mixing conditions but variable composition). The crystallization temperature T_c taken as the maximum of the crystallization curve at a cooling rate of 10 °C/min was at 140 °C for the pure PVDF and at 178 °C with a shoulder at the high temperature side for the pure PA-6. The crystal modifications formed are then, as confirmed by WAXS and melting point measurements, the α-form of PVDF and, in the case of PA-6, mainly the γ-modification and, to a smaller extent, the α-form. The maximum of the DSC melting peak is located at 175 °C for PVDF and at 215 °C and 222 °C for PA-6.

The most striking results of these investigations has been found with the crystallization of the 85/15 blend. It is remarkable that it showed only one crystallization exotherm at 140 °C, that is, at the T_c of PVDF, whereas nothing happened at the usual PA-6 crystallization temperature. Nevertheless, the DSC heating curve of this blend exhibited the usual melting endotherms of the two polymers (cf. Fig. 7). WAXS- and IR-analyses confirmed that the PA-6 crystallized in this blend.

In some of the samples, the introductory referred fractionated crystallization occurred. In the 70/30 and 50/50 blends, the PA-6 crystallizes partly at 184 °C (that is, at a somewhat higher temperature than in the pure material) and partly at 140 °C (that is, as in the 85/15 blend) as derived from comparison of the exotherm and the endotherm peak areas. In the 50/50 blend, also the crystallization of the PVDF component split into two steps at 140 °C and 116 °C. In the 15/85 blend, the PVDF crystallized merely at the low temperature step at about 112 °C.

Variations of the cooling rates by a factor of two resulted in small shifts of T_c of about 3 °C for PVDF and of about 4 °C for PA-6. The variation of the cooling rate, however, did not affect the number and the relative intensities of the crystallization peaks. In particular, the unusual, complete coincidence of T_c in the 85/15 blend occurred at several cooling rates ranging between 0.5 °C/min and 100 °C/min.

In Fig. 6, the crystallization in dependence on the extrusion cycle number, that is, in dependence on the mixing intensity, for a fixed composition is shown. The DSC cooling curve of the four-times extruded 75/25 blend exhibited again the coincident crystallization of the PVDF matrix and the PA-6 droplets at 140 °C. Additionally, in the case of the one-time extruded blend, a part of the PA-6, possibly the greater domains, crystallized at its usual T_c of 184 °C, and a part of the PVDF, probably the droplets dispersed inside the referred PA-6 domains, crystallized at 113 °C. With increasing number of extrusion cycles, the PA-6 domains became smaller and lost their composed character. This, obviously, caused the disappearence of the usual high temperature crystallization peak of

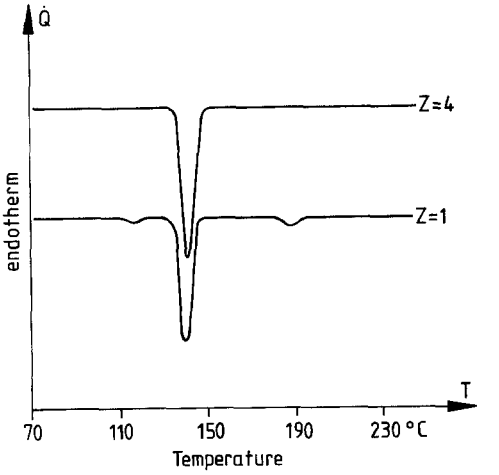

Fig. 6. DSC crystallization curves of the PVDF/PA-6 = 75/25 vol.-% blend; cooling rate: 10 °C/min; parameter: number of extrusion cycles Z

the PA-6, as well as that of the low temperature crystallization peak of the PVDF which, therefore, represents the crystallization of the dispersed, smaller PVDF droplets. Obviously, the described effects, in particular the fractionation of the crystallization, depend to a large extent on the dispersion of the minor component. With increasing dispersitivity of that component, the magnitudes of its additional crystallization peaks become stronger at the expense of the usual peak.

Figures 7 and 8 display the DSC crystallization and melting temperatures, and the melting enthalpies of the four-times extruded blends in dependence on the composition. The composition ranges in which fractionated crystallization occurred for the four-times extruded samples can be read from these figures. The PVDF melting points, as well as WAXS analysis indicated that this component crystallized in every case in its α-modification.

The relative crystallinity of each component did not alter significantly with composition and extrusion cycle number.

3.2.2. PVDF/PBTP blends

The unblended PBTP crystallized at about 180 °C as revealed by DSC (Fig. 9). After adding 15 vol.-% PVDF, the T_c rose remarkably to 189 °C and 194 °C for the one-, and for the four-times extruded blends, respectively. Similarly, the pure PVDF crystallized at 140 °C, whereas the corresponding T_c in the blends was between 142 °C and 148 °C. In particular, in the 15/85 blend, the PVDF crystallized at 147 °C after one extrusion cycle whereas it crystallized at 143 °C after four. In the four-times extruded 85/15 blend, the PBTP crystallization was suppressed in a similar manner as already described for the PA-6. The PBTP crystallized at 147 °C simultaneously with the PVDF as derived from comparison of the exotherm and the endotherm DSC peaks of the cooling and reheating runs.

The melting temperature of PBTP is 225 °C in the 0/100 and 15/85 blends, and 222 °C in the 85/15 blend.

As derived from the DSC melting temperatures of about 174 °C and from WAXS analysis, also in these blends, the PVDF has crystallized in its α-modification.

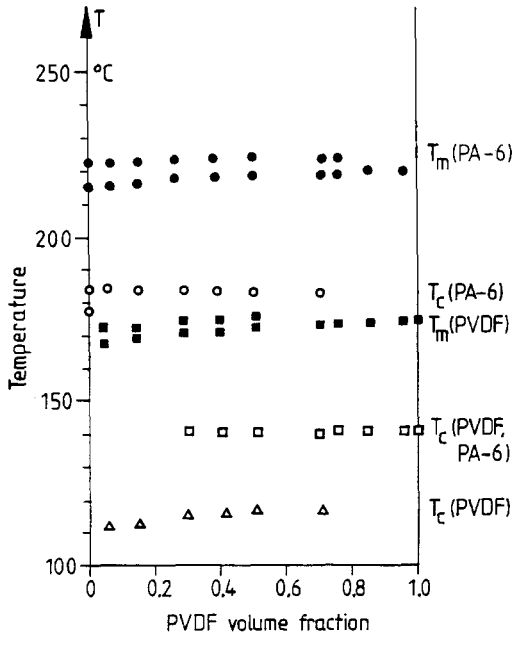

Fig. 7. DSC crystallization and melting temperatures of the PVDF/PA-6 blends; four extrusion cycles

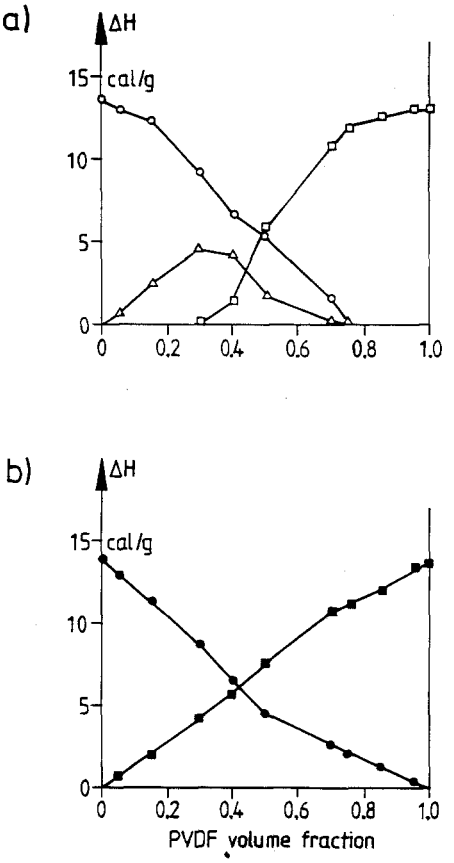

Fig. 8. DSC crystallization (a) and melting (b) enthalpies of the four-times extruded PVDF/PA-6 blends; meaning of symbols is the same as in Fig. 7

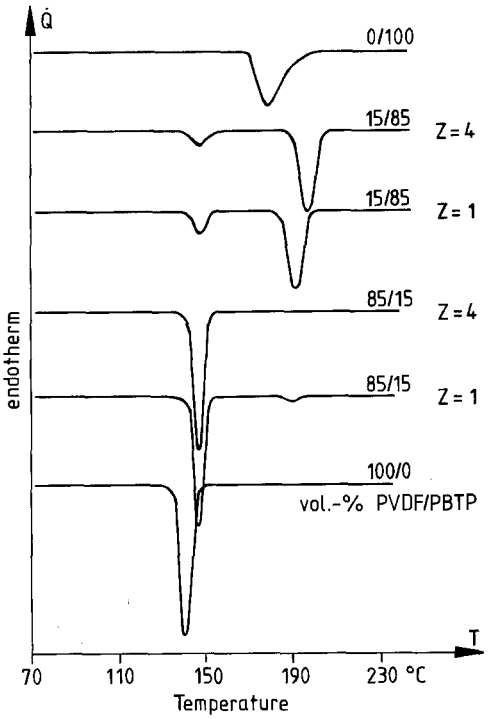

Fig. 9. DSC crystallization curves of PVDF/PBTP blends. Cooling rate: 10 °C/min; parameters: blend composition and number of extrusion cycles Z

4. Discussion

The crystallization and melting of the investigated blends exhibits several differences to that of the pure components. The occasional occurrence of double-melting endotherms of the components during the reheating runs and the melting point depressions of the minor component can be explained in the usual way by imperfect crystal formation during the – possibly fractionated – crystallization, by molecular reorganization and lamellar thickening during heating, and, in the case of the PA-6, by polymorphism [36–42]. These two issues will, therefore, no longer be considered in the following. In contrast, the following issues require a profound treatment:

1. splitting of the crystallization of the dispersed component into several distinct steps ("fractionated crystallization", both PVDF and PA-6 in their blends);

2. complete coincidence of the crystallization of the dispersed component with the matrix crystallization (both PA-6 and PBTP in their blends with PVDF);

3. remarkable rise in crystallization temperature after adding a second component (PA-6 and PBTP in their PVDF blends and PVDF in its PBTP blends).

These effects are partly connected with the dispersion of the component under investigation into the other and they are enhanced if this dispersion becomes finer.

4.1. Retarded and/or fractionated crystallization of the dispersed component

Let us turn to the first effect as listed at the beginning of this chapter, that is, to the fractionated crystallization of PVDF and PA-6 in their blends.

It is important for the following considerations to point out that the crystal growth rates of all components amount to at least 10 μm/min in the temperature range where the crystallization steps occur [6, 43]. Therefore, a nucleated dispersed particle crystallizes promptly, and the primary rather than the secondary nucleation is the rate-controlling factor of the crystallization kinetics of the dispersed phase. For the same reason, the crystallization temperatures as observed in the DSC cooling run agrees roughly with the nucleation temperature.

It is well known that polymers generally crystallize heterogeneously nucleated when cooling from temperatures well above the melting temperature. The free energy ϕ^* of formation of a rectangular nucleus of critical size at an undercooling ΔT is given by [34, 44, 45]

$$\phi^* = 16\,\Delta y_{ps}\, y_p(m,c)\, y_p^e(m,c)\, (T_m^o/(\Delta T\, \Delta H_f f))^2 \quad (1)$$

where the "specific interfacial energy difference" Δy_{ps} is given by

$$\Delta y_{ps} = y_p(m,c) - y_{ps}(m) + y_{ps}(c)\ ^{1}). \quad (2)$$

Here, $y_{ps}(m)$ and $y_{ps}(c)$ are the interfacial energies between the nucleating substrate and the polymer melt and crystals, respectively. $y_p(m,c)$ and $y_p^e(m,c)$ are the surface free energies parallel and perpendicular to the molecular chain direction between the crystal and its own melt, respectively. ΔH_f is the heat of fusion per unit volume, and $f = 2T/(T_m^o + T)$ is a correction

[1]) For the sake of standardization throughout this paper, the terms "surface energy" and "interface energy" are used, whereas in the literature the use of the term "tension" instead of "energy" is customary. Furthermore, the convention $y_{12}(1,2) = y_{\text{component "1", component "2"}}$ (state of component "1", state of component "2") is introduced. m = melt, a = amorphous, c = crystal, s = substrate, and p = polymer.

factor for the bulk free energy difference between the supercooled liquid and the crystal. T_m^o is the equilibrium melting temperature. The relation

$$\Delta y_{ps} = 2y_p(m, c) \tag{3}$$

holds for homogeneous nucleation.

If one assumes that ϕ^*/kT must be smaller than a certain critical value for the onset of the crystallization, and neglecting that the crystallization rate depends also on the temperature dependent mobility of the crystallizable segments, then the following approximate relation holds between Δy and the undercooling at which the nucleation by two different species "1" and "2" gives rise to crystallization

$$\Delta y_1/\Delta y_2 \approx (T_1/T_2)\,(\Delta T_1/\Delta T_2)^2\,. \tag{4}$$

The inversion of this statement is also true. The temperature at which a certain heterogeneity induces crystallization depends on its Δy-value (Fig. 10). Usually, only that heterogeneity with the smallest Δy-value is efficient; via secondary nucleation at the created crystals, the crystallization process spreads over the whole volume if it has started anyway, and it has completed before the undercooling of the heterogeneity with the second smallest Δy-value is reached. It is exactly this that is inhibited if the material volume is divided into many separated droplets as in some of our samples.

Among a large number of small polymer droplets each of volume v_D, the fraction of droplets containing exactly z heterogeneities of the kind "1" that initially induced crystallization follows a Poisson distribution function [46]:

$$f_z^{(1)} = [M^{(1)}v_D)^z/z!]\,\exp\,(-\,M^{(1)}v_D) \tag{5}$$

where $M^{(1)}$ is the concentration of randomly suspended heterogeneities and $M^{(1)}v_D$ is their mean number per droplet. The fraction of droplets containing at least one heterogeneity of the kind "1" is given by $f_{z>o}^{(1)} = 1 - f_0^{(1)}$ and amounts to

$$f_{z>0}^{(1)} = 1 - \exp\,(-\,M^{(1)}v_D)\,. \tag{6}$$

The consideration of a droplet size distribution may somewhat modify this equation. $f_{z>0}^{(1)}$ describes that part of the droplets and, therefore, of the material that crystallizes induced by heterogeneity "1". The remainder crystallizes at a greater undercooling induced by heterogeneity "2" and so on. For these further crystallization steps the same considerations hold. Since $f_{z>0}^{(i)}$ depends on v_D, the influence of the dispersitivity on the relative strength of the different crystallization steps is obvious. For sufficient large droplets, $f_{z>0}^{(1)}$ is near one and no fractionated crystallization occurs. On the contrary, a certain crystallization step is suppressed (or undetectable) if the relation

$$M^{(i)}v_D \ll 1 \tag{7}$$

holds. From the relative intensity of the different crystallization steps, conclusions can be drawn on the concentration of the respective heterogeneities if the mean size of the droplets is known. This will be done next.

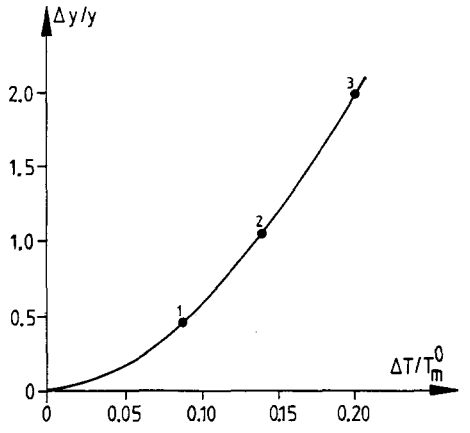

Fig. 10. Plot of the relative specific interfacial energy difference $\Delta y/y$ against the relative undercooling $\Delta T/T_m^o$ at which a heterogeneity nucleates the polymer. Combining Eqs. (3), (4), and (8), it turns out that $\Delta y_{ps}/y_p(m, c) = 62.5\,(T/T_m^o)\,(\Delta T/T_m^o)^2$. "1", "2": two different heterogeneous nucleations; "3": homogeneous nucleation

4.2. Estimation of nuclei concentrations

The average volumes v_D of the dispersed PA-6 particles in the four-times extruded PVDF/PA-6 85/15 and 75/25 blends amount to about 4×10^{-15} cm^3 and 3×10^{-14} cm^3, respectively, as calculated from the geometric mean of the minimal and maximal particle sizes. Because the PA-6 droplet crystallization is almost completely suppressed at the usual temperatures, the relation $M^{(1)}v_D \ll 1$ must hold where $M^{(1)}$ is the number density of nucleating impurities active in PA-6 above 140 °C. Followingly $M^{(1)}$ should be less than 10^{13} cm^{-3} which agrees roughly with the number density $(0.2 \ldots 2) \times 10^{12}$ cm^{-3} of spherulites and sheaves grown in pure PA-6 at 140 °C.

On the contrary, in the one time extruded 85/15 and 75/25 blends, the PA-6 particles are much larger and PA-6 fibers are still present. Accordingly, there is only a split up of the PA-6 crystallization, and the DSC peak at about 180 °C does not vanish as for the four-times extruded blend.

The average volume of a PVDF particle in the PVDF/PA-6 = 15/85 blend after four extrusion cycles amounts to about 8×10^{-15} cm^3. Moreover, all of them crystallize at the low temperature step. Followingly, the number density $M^{(1)}$ of the nucleating impurities which are active in PVDF at 140 °C is below about 5×10^{13} cm^{-3}. Nevertheless, in the 50/50 blend, there are also larger PVDF particles with a volume of about 4×10^{-12} cm^3, the crystallization of which most probably gives rise to the DSC peak at 140 °C since the probability of containing a heterogeneity is greater for a large particle. Therefore, $M^{(1)}$ should amount at least to 2×10^{11} cm^{-3}.

In the PVDF/PBTP = 85/15 blend, the average volume of dispersed PBTP particles after the first and the fourth extrusion cycles amount to about 4×10^{-12} cm^3 and 5×10^{-14} cm^3, respectively. The strong decrease of the T_c of the dispersed PBTP droplets even for a part of the one time extruded blend suggests that the number density of the heterogeneities which nucleate PBTP above 148 °C is below about 2×10^{11} cm^{-3}.

The foregoing estimations of $M^{(i)}$ are summarized in Table 2.

4.3. Estimation of specific interfacial energies for PVDF nuclei

By Eq. (4), one can conclude the relative Δy-values of the heterogeneities from the corresponding undercoolings. With less accuracy, even the absolute values can be calculated as will be done for PVDF in the following. For this sake, use is made of the fact that homogeneous nucleation of a wide range of anorganic and organic substances including polymers often occurs at

$$T_c^{\text{hom}} \approx 0.8\, T_m^o \tag{8}$$

[34]. With T_m^o (α-PVDF) = 459 K (186 °C) [39] and T_m^o (γ-PA-6) = 500 K (227 °C) [31, 43], one gets T_c^{hom} = 367 K (94 °C) for PVDF and 400 K (127 °C) for PA-6. Both these values are well below the T_c observed for all fractions and components in our blends which, therefore, in every case must crystallize heterogeneously nucleated. At a low cooling rate of 1 °C/min, the temperatures of the fractionated crystallization of PVDF are 148 °C and 119 °C. With $y_{\text{PVDF}}(m, c) = 9.7$ mJ/m^2 [6, 47], and using Eqs. (3) and (4), we obtain for the specific interfacial energy differences of the two nucleating heterogeneities $\Delta y_{\text{PVDF, s1}}$ (148 °C) = 3.8 mJ/m^2 and $\Delta y_{\text{PVDF, s2}}$ (119 °C) = 11 mJ/m^2 (Table 2).

Table 2. Calculated nucleation and interfacial data

	PVDF	PA-6	PBTP
$M^{(i)}$ [cm^{-3}]			
$i = 1$	$2 \times 10^{11} \ldots 5 \times 10^{13}$	$< 10^{13}$	$< 2 \times 10^{11}$
Δy_{psi} [mJm^{-2}]			
$i = 1$ (at 148 °C)	3.8		
$i = 2$ (at 119 °C)	11		
$i = 3$ (with c-PA-6)	4.2		
$y_{\text{PVDF, PA-6}}$ [mJm^{-2}]			
(c, m)	4.1		
(c, c)	0.2		

4.4. Coincidence of crystallization temperatures

4.4.1. PVDF/PA-6

The crystallization in the blends studied is remarkable not only since the crystallization of the dispersed phase at its usual temperature is sometimes completely supressed, but also since that delayed crystallization then occurs completely simultaneously with that of the matrix. The coincidence of the crystallization of the finely dispersed part of PA-6 with the PVDF matrix crystallization at 140 °C, in particular, indicates a nucleating efficiency either of PVDF crystals on the PA-6 melt, or of PA-6 crystals on the PVDF melt. In view of the nonaltered T_c of PVDF, we suppose that the PVDF crystallization induces the PA-6 crystallization rather than vice versa. The crystals of the PVDF matrix, followingly, act as nucleating heterogeneity with the second lowest Δy-value for PA-6.

As already mentioned, a low interfacial energy between substrate and growing crystal is promotive of a nucleating activity. The interfacial energy of two polymers can roughly be estimated by the harmonic-mean method proposed by Wu [1, 48]

$$y_{12} = y_1 + y_2 - 4y_1^d y_2^d/(y_1^d + y_2^d) - 4y_1^p y_2^p/(y_1^p + y_2^p) \tag{9}$$

where y_j, y_j^d, and y_j^p are the surface energy and its dispersive and polar fractions, respectively, of poly-

mer j. For the amorphous phase, we have [48] $y_{PVDF}(a) = 36.5$ mJ/m^2, $y^p_{PVDF}(a) = 13.7$ mJ/m^2, $y_{PA\text{-}6}(a) = 42$ mJ/m^2, and $y^p_{PA\text{-}6}(a) = 14$ mJ/m^2.

The surface energy of a polymeric crystal $y_p(c)$ can be estimated by [48]

$$y_p(c) = y_p(a)\ (\varrho_p(c)/\varrho_p(a))^n \tag{10}$$

where $\varrho_p(c)$ and $\varrho_p(a)$ are the crystalline and amorphous densities and n is a constant which amounts to about 4. With $\varrho_{PVDF}(a) = 1.68$ g/cm^3 [49], $\varrho_{\alpha\text{-}PVDF}(c) = 1.92$ g/cm^3 [50], $\varrho_{PA\text{-}6}(a) = 1.09$ g/cm^3, and $\varrho_{\gamma\text{-}PA\text{-}6}(c) = 1.19$ g/cm^3 [40], all at 20 °C, it turns out that $y_{\alpha\text{-}PVDF}(c) = 62.3$ mJ/m^2 and $y_{\gamma\text{-}PA\text{-}6}(c) = 59.7$ mJ/m^2. The temperature dependence of the surface energy of the amorphous phase amounts to $dy(a)/dT = -$ (0.05 ... 0.08) mJ/(m^{2}K) for most polymers [48]. Because, additionally, dy/dT is proportional to the thermal expansion coefficient which is less for the crystalline phase, the surface energies of the crystalline phases at the T_c of 140 °C are only a few mJ/m^2 lower than those at 20 °C. Then, by Eq. (8), the interfacial energies between the PVDF crystal and the PA-6 melt and between the PVDF and the PA-6 crystalline phases amount to $y_{PVDF,\,PA\text{-}6}(c, m) = 4.1$ mJ/m^2 and $y_{PVDF,\,PA\text{-}6}(c, c) = 0.2$ mJ/m^2, the difference of which may account for the nucleating activity of the crystalline PVDF.

Beside the low amount of the interfacial energy, nucleation is possibly favored by the matching of the lattice surfaces lateral to the chain directions. The dimensions of the unit cell of the monoclinic α-modification of PVDF amount to $a = 0.496$ nm, $b = 0.964$ nm, and $c = 0.462$ nm [50]. The orthorhombic unit cell of the γ-modification of PA-6 is characterized by $a = 0.482$ nm, $b = 0.782$ nm, and $c = 1.67$ nm [40, 51]. The mismatching of c_{PVDF} and $a_{PA\text{-}6}$ and of $3a_{PVDF}$ and $c_{PA\text{-}6}$ amounts to 4 % and 11 %, respectively, both of which are within the 15 %-disparity of lattice periodicities stated as limiting upper bound of epitaxial growth [52].

If the nucleating activity of the PVDF crystals for the crystallization of PA-6 is indeed epitaxially supported, one could, vice versa, expect a nucleating efficiency of PA-6 crystals for PVDF too, which then would be indicated by the low-T_c of PVDF. With Eq. (2), however, using the interfacial energies $y_{PVDF}(m, c) = 9.7$ mJ/m^2, $y_{PA\text{-}6,PVDF}(c, m) = 5.7$ mJ/m^2, $y_{PA\text{-}6,PVDF}(c, c) = 0.2$ mJ/m^2, one gets $\Delta y_{PVDF,PA\text{-}6} = 4.2$ mJ/m^2 which is significantly lower than the value of 11 mJ/m^2 which was estimated by use of Eq. (4) for the heterogeneity which nucleates PVDF at the low temperature step and which we possibly overestimated assuming a too high value of T_c^{hom}.

4.4.2. PVDF/PBTP

The coincident crystallization of the PVDF matrix and dispersed PBTP particles in the 85/15 blend ($Z = 4$) indicates a nucleating efficiency between the components. Their crystallization processes take place at (142...148) °C that is above the T_c of pure PVDF. It is not clear whether the PVDF or the PBTP crystallizes first. The nucleation of the first crystallizing component may be induced either by a species of nucleating heterogeneities or by the molten second blend component. Whereas it is not evident which of both substances is nucleated first, the coincidence of the T_c indicates that the crystallizing component acts as nucleating substrate for the other component.

4.5. Rise of the T_c of the continuous phase

Let us turn, finally, to the promoted crystallization of PA-6 and PBTP as indicated by the rise of their T_c if they constitute the matrix phase in their blends with PVDF. This effect can be due to two features. First, it may arise from a decrease of the glass temperature T_G of the crystallizing component (PA-6 or PBTP) in the interfacial regions with the low-T_g component PVDF. The interface in the melt is relatively broad as indicated by the high level of dispersion which, in turn, is caused by a small interfacial energy. The increase of the segment mobility of PA-6 and PBTP in the interfacial layers which contribute remarkably to the overall crystallization due to their high thickness and the high degree of dispersitivity may prevail against both the retardation of formation of secondary nuclei [7, 8] and the energy dissipation due to rejection [4, 17, 18] of dispersed PVDF particles by growing spherulites of the matrix phase.

Alternatively, the rise of the T_c may be caused by migration of nucleating heterogeneities from PVDF toward PA-6 and PBTP, respectively, the latter two exhibiting slightly higher surface energies than PVDF [48]. Nucleating impurities like inorganic compounds generally exhibit high energy surfaces [48]. The tendency of a system to minimize the interfacial energies would favour the migration of these heterogeneities across the phase border [22, 53] toward that component with the higher surface energy. In this way, the density of nuclei in PA-6 and PBTP in their blends with

PVDF would increase which could account for the rise of their T_c.

The increase of the T_c of the continuous PVDF phase in the blends with PBTP may arise from a nucleating efficiency of the amorphous or the crystalline phase of PBTP.

We have observed the drop of the T_c of the dispersed components and the coincidence of crystallization of the PVDF matrix and the dispersed phase in blends of PVDF with the PA-6 of another manufacturer, and in blends with PA-6.6 too, all these systems exhibiting a high level of dispersion.

5. Conclusions

The work reported here has shown that the phenomenon of fractionated crystallization can concern both components when forming the dispersed phase. In the case of the one-time extruded PVDF/PA-6 75/25 blend, even the major component PVDF crystallizes fractionated due to the several levels of dispersion realized (insertion of matrix material into particles of the dispersed component). Owing to the extended range of undercoolings accessible for PA-6 and PBTP in their blends with PVDF, provided they are finely dispersed, usually hidden nucleating activities of PVDF crystals for PA-6 as well as between PVDF and PBTP become effective, leading to a coincident crystallization of both blend components. The PVDF/PBTP blends exhibit possibly a novel mutual nucleation behavior in crystallizable polymer blends: a molten component serves as nucleating substrate for the second component and then itself becomes nucleated by the crystalline phase of that component.

Acknowledgements

Financial support by the Arbeitsgemeinschaft Industrieller Forschungsvereinigungen (AIF grant No. 47/86) is gratefully acknowledged.

References

1. Paul DR, Newman S (eds) (1978) Polymer Blends. Academic Press, New York
2. Olabisi O, Robeson LM, Shaw MT (1979) Polymer – Polymer Miscibility. Academic Press, New York
3. Nishi T (1985) CRC Crit Rev Solid State Mater Sci 12(4):329
4. Martuscelli E (1984) Polym Eng Sci 24:563
5. Alfonso GC, Russell TP (1986) Macromolecules 19:1143
6. Wang TT, Nishi T (1977) Macromolecules 10:421
7. Calahorra E, Cortazar M, Guzman GM (1982) Polymer 23:1322
8. Martuscelli E, Sellitti C, Silvestre C (1985) Makromol Chem Rap Comm 6:125
9. Bartczak Z, Martuscelli E (1987) Makromol Chem 188:445
10. Marinow S, May M, Hoffmann K (1983) Plaste & Kautschuk 30:620
11. Paul DR, Barlow JW, Bernstein RE, Wahrmund DC (1978) Polym Eng Sci 18:1225
12. Eder M, Wlochowicz A (1984) Acta Polym 35:548
13. Morris MC (1967) Rubber Chem Techn 40:341
14. Ghijsels A (1977) Rubber Chem Techn 50:278
15. Lipatov YS, Lebedev EV (1979) Makrom Chem Suppl 2:51
16. Kishore K, Vasanthakumari R (1986) Polymer 27:337
17. Keith HD, Padden Jr FJ (1963) J Appl Phys 34:2409
18. Bartczak Z, Galeski A, Martuscelli E (1984) Polym Eng Sci 24:1155
19. Hsu CC, Geil PH (1987) Polym Eng Sci 27:1542
20. Chatterjee AM, Price FP, Newman S (1975) J Polym Sci Phys Ed 13:2369, 2385, 2391
21. Lotz B, Wittmann JC (1986) J Polym Sci Phys Ed 24:1559
22. Bartzcak Z, Galeski A, Pracella M (1986) Polymer 27:537
23. Ghijsels A, Groesbeek N, Yip CW (1982) Polymer 23:1913
24. O'Malley JJ, Crystal RG, Erhardt PF (1969) Am Chem Soc Div Polym Chem Polym Prepr 10(2):796
25. Lotz B, Kovacs AJ (1969) ibid, p 820
26. Robitaille C, Prud'homme J (1983) Macromolecules 16:665
27. Aref-Azar A, Hay JN, Marsden BJ, Walker N (1980) J Polym Sci Phys Ed 18:637
28. Baitoul M, Saint-Guirons H, Xans P, Monge P (1981) Europ Polym J 17:1281
29. Tsebrenko MV (1983) Int J Polym Mater 10:83
30. Klemmer N, Jungnickel B-J (1984) Colloid Polym Sci 262:381
31. Koutsky JA, Walton AG, Baer E (1967) J Appl Phys 38:1832
32. Cormia PL, Price FP (1962) J Chem Phys 37:1333
33. Burns JR, Turnbull D (1966) J Appl Phys 37:4021
34. Wunderlich B (1976) Macromolecular Physics, Vol 2, Crystal Nucleation – Growth – Annealing. Academic Press, New York San Fancisco London
35. Barham PJ, Jarvis DA, Keller A (1982) J Polym Sci Phys Ed 20:1733
36. Lovinger A (1982) In: Bassett DC (ed) Developments in Crystalline Polymers Vol 1. Appl Sci Publ, London New Jersey
37. Osaki S, Ishida Y (1975) J Polym Sci Phys Ed 13:1071
38. Yadav YS, Jain PC (1986) J Macr Sci – Phys B25:335
39. Chen CT, Frank CW (1984) Ferroelectrics 57:51
40. Illers KH, Haberkorn H, Simak P (1972) Makromol Chem 158:285
41. Weigel P, Hirte R, Ruscher C (1974) Faserf Textilt 25:198, 283
42. Hirami M (1984/85) J Macr Sci – Phys B23:397
43. Magill JH (1962) Polymer 3:655
44. Price FP (1969) In: Zettlemoyer AC (ed) Nucleation. Marcel Dekker, New York, chap 8
45. Lovinger AJ, Davis DD, Padder Jr FJ (1985) Polymer 26:1595
46. Pound GM, LaMer VK (1952) J Am Chem Soc 74:2323
47. Mancarella C, Martuscelli E (1977) Polymer 18:1240
48. Wu S (1982) Polymer Interface and Adhesion. Marcel Dekker, New York
49. Nakagawa K, Ishida Y (1973) Kolloid Z Z Polym 251:103
50. Hasegawa R, Takahashi Y, Chatani Y, Tadokoro H (1972) Polym J 3:600
51. Bradbury EM, Brown L, Elliott A, Parry DAD (1965) Polymer 6:465

52. Mauritz KA, Baer E, Hopfinger AJ (1978) J Polym Sci Macromol Rev 13:1
53. Bartczak Z, Galeski A, Martuscelli E, Janik H (1985) Polymer 26:1843

Received January 28, 1988;
accepted August 5, 1988

Authors' address:

H. Frensch
Deutsches Kunststoff-Institut
Schloßgartenstr. 6R
D-6100 Darmstadt, F.R.G.